Supporting Information to "Hierarchical self-assembly of patchy colloidal platelets"

Carina Karner,* Emanuela Bianchi,† and Christoph Dellago‡
Faculty of Physics, University of of Vienna, Boltzmanngasse 5, A-1090, Vienna, Austria
(Dated: February 20, 2020)

I. BARYCENTRIC COORDINATES

With the help of barycentric coordinates it is possible visualize mixtures of three components p_l, p_m, p_c that fulfill $p_l + p_m + p_c = 1$. This requirement is given in our case where p_i, with $(i = l, m, c)$ are the yields of the different cluster types. For ma-systems, p_l is the yield of clusters with $N < 3$, p_m is the micelle yield, and p_c is the yield of non-micelle clusters with $N \geq 3$. To use barycentric coordinates in mo-systems, we need to map the yield of four cluster types to the three components p_i. As 5-stars and 6-stars are dominant at different Δ-values we decided on the following mapping: for $\Delta = 0.2$, p_l corresponds to the yield of clusters with $N < 5$, p_m is the yield of micelle clusters with $N = 5$, while all non-5-star clusters with $N \geq 5$ map to p_c; in contrast for all $\Delta > 0.2$, p_l represents all clusters with $N < 6$, p_m is the yield of micelle clusters with $N = 6$, and p_c encompasses all non-6-star clusters with $N \geq 6$.

With these definitions, (p_l, p_m, p_c) are mapped onto a equilateral triangle. Each triangle vertex corresponds to the case where one $p_i = 1$, and the others are 0, whereas more mixed yields are represented by points within the triangle. If we set the Cartesian triangle edge points to be $x_l = (0, 0)$, $x_c = (1, 0)$ and $x_m = (1/2, \sqrt{(3)}/2)$, the barycentric vector q_t is given by

$$q_t = (\frac{1}{2} \cdot (2p_c + p_m), \frac{\sqrt{(3)}}{2} \cdot p_m) \quad (1)$$

The equilateral triangle subsequently split into 9 equilateral triangles and the colors of the edge triangles blue, pink and yellow denote the case where one one cluster type has a yield higher than 2/3. In the case of mixed systems where no cluster type is 2/3 dominant, the set (p_l,p_m,p_c) maps to points closer to the triangle center and the adopted color corresponds to the respective inside triangles.

II. HISTOGRAMS OF YIELDS

We calculate the yields of the liquid state, the micelles and the chains/loops for all particle classes (manta (ma) and mouse (mo)) and all topologies (symmetric (s) and asymmetric (as)). See the main paper for definitions of the liquid state, the micelles, and the chain/loop clusters. The yields for all pairs (Δ, ϵ) are summarized in the histograms in Fig. 1a, 2a, 3a and 4a. With barycentric coordinates (see Sec.I) we map the yields to heatmaps displayed in Fig. 1b, 2b, 3b and 4b as well as in Fig. 2c/h and 3c/h in the main paper. The respective barycentric color triangles are displayed in Fig. 1c, 2c, 3c and 4c and Fig. 2b/f/g and 3b/f/g in the main paper.

III. DESIGN STRATEGIES FOR STAR LATTICES

We observe that in contrast to boxes, stars do not yield an extensive hexagonal lattice at second stage assembly. We identify three factors that lower the star yield and therefore hamper the formation of long range hexagonal order in stars.

Firstly, the highest star yield with ≈ 0.75 is lower than the yields for boxes and open boxes with over 0.9. Besides stars, assembly products for mo-s systems contain other clusters that destroy the star lattice order: these clusters are not fully formed stars, p-bonded dimers (labeled as 2p-off in Fig. 6) and broken stars (labeled as 6np-on&p-off in Fig. 6). Broken stars are 5- or 6-particle clusters where parts of the star are shifted and yield parallel and dangling bonds instead of 5 (5-stars) or 6 (6-stars) non parallel bonds (see Fig. 6a). Hence one strategy to reduce the yield of p-bonded dimers and broken stars is to generally disfavor p-bonds.

Another effect that lowers the yield might be the competition with chains: we observe that stars only become prevalent in regions of the interaction strength where chains start to compete with stars, *i.e.*, at $\epsilon > 9.2k_BT$. Hence, disallowing p-bonds could extend the prevalence region of stars to higher interaction strengths and to $\Delta > 0.5$, and in absence of chains higher top yield could be reached.

Lastly, during compression of the NPT runs, stars, especially 5-stars tend to get destroyed and become broken stars, that in return destroy the long range order.

Summarizing, the most apparent strategy to get a higher star yield and subsequently long range star lattices is to disfavour p-bonds. One way to achieve that is to change patch specificities. Instead of one type of patch where patches always attract each other with $-\epsilon$, we propose two types of patches, where patches of the same kind repel each other with $+\epsilon$, while differing patches attract each other with $-\epsilon$. This scenario disfavors p-bonds and broken stars become unfavorable (see Fig. 6b). Additionally, as p-bonds are generally disfavored, chains, which

*Electronic address: carina.karner@univie.ac.at
†Electronic address: emanuela.bianchi@tuwien.ac.at
‡Electronic address: christoph.dellago@univie.ac.at

need p-bonds, become disfavorable as well. Hence, this might lead to an extended range in the (Δ, ϵ) plane where stars are the dominant self assembly product.

IV. FIGURES

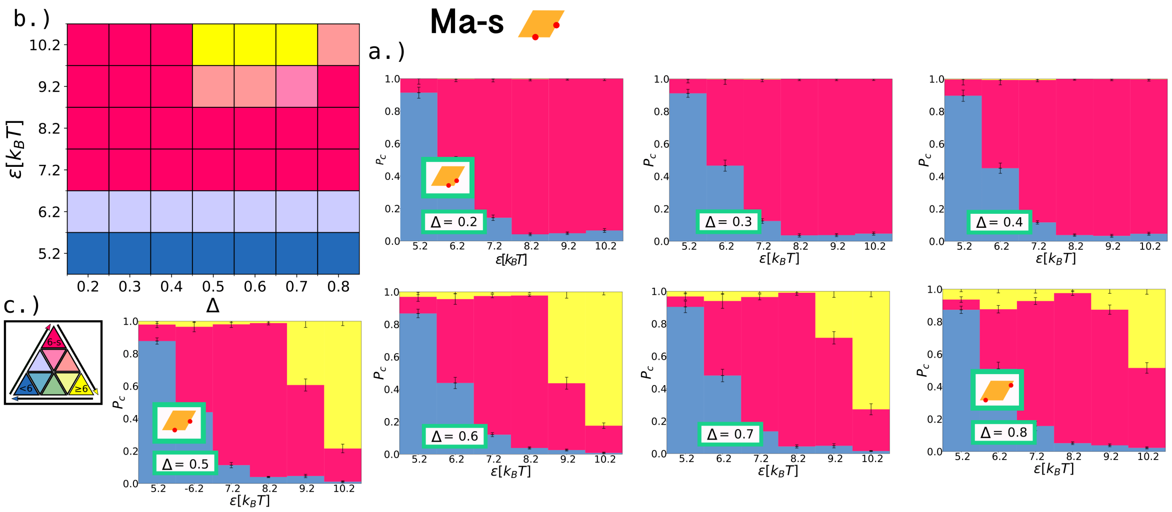

FIG. 1: Yield histograms and heatmaps for symmetric manta systems (ma-s). **a.)** histograms of yields for the cluster types liquid (blue), boxes (pink) and chain/loops (yellow). See the main paper for the definitions of the cluster types. There is one histogram plot for each patch position Δ, the x-axis of each of these histograms denotes the interaction strength ϵ. **b.)** The heatmap summarizes all yield histograms through mapping the yield distributions for each (Δ, ϵ) to a barycentric color triangle. **c.)** The barycentric color triangle for ma-s.

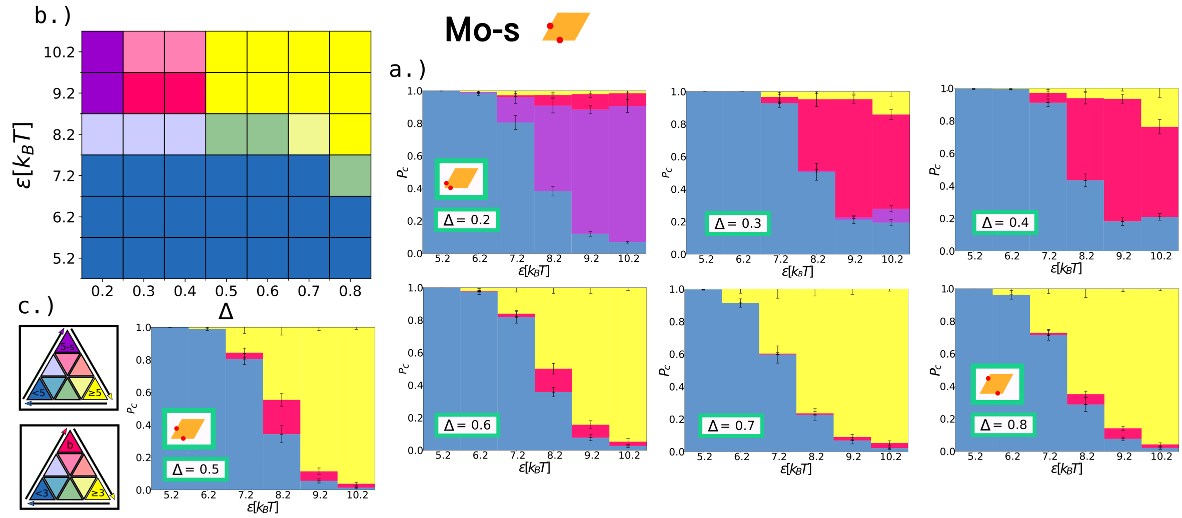

FIG. 2: Yield histograms and heatmaps for symmetric mouse systems (mo-s). **a.)** histograms of yields for the cluster types liquid (blue), 6-stars (pink), 5-stars (purple) and chain/loops (yellow). See the main paper for the definitions of the cluster types. There is one histogram plot for each patch position Δ, the x-axis of each of these histograms denotes the interaction strength ϵ. **b.)** The heatmap summarizes all yield histograms through mapping the yield distributions for each (Δ, ϵ) to a barycentric color triangle. **c.)** The barycentric color triangles for mo-s, where the upper triangle is used only to map the histogram of $\Delta = 0.2$, and the lower triangle is used for all other Δ-values.

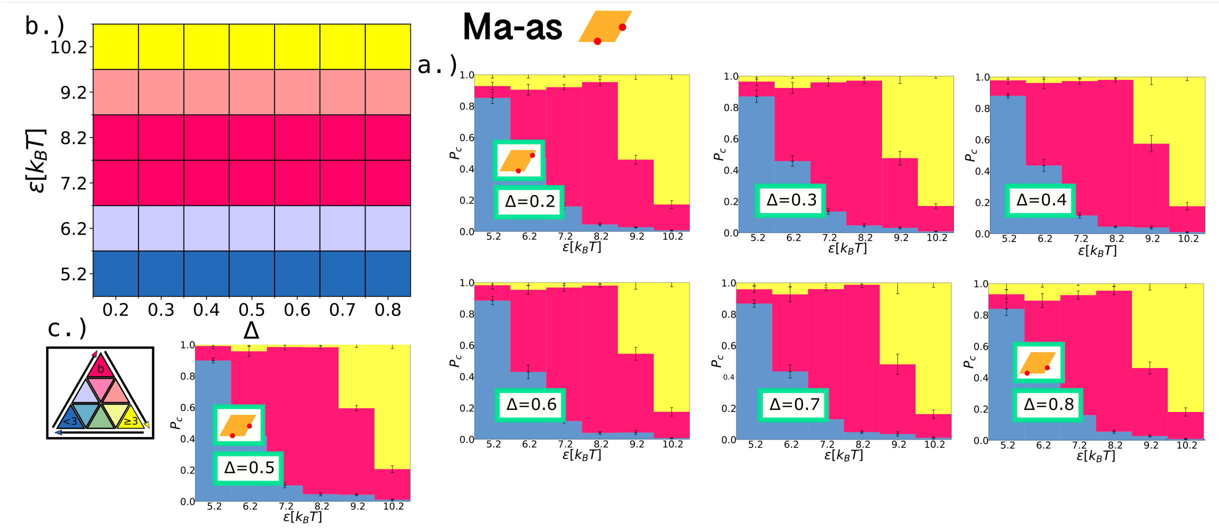

FIG. 3: Yield histograms and heatmaps for asymmetric manta systems (ma-as). **a.)** histograms of yields for the cluster types liquid (blue), open boxes (pink) and chains/loops (yellow). See the main paper for the definitions of the cluster types. There is one histogram plot for each patch position Δ, the x-axis of each of these histograms denotes the interaction strength ϵ. **b.)** The heatmap summarizes all yield histograms through mapping the yield distributions for each (Δ, ϵ) to a barycentric color triangle. **c.)** The barycentric color triangle for ma-as.

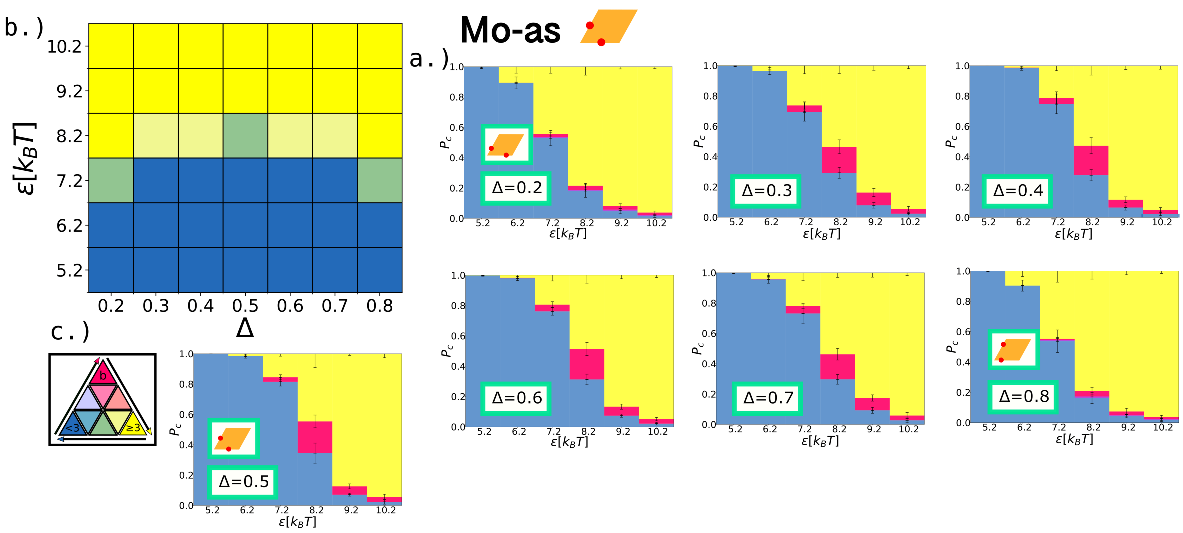

FIG. 4: Yield histograms and heatmaps for asymmetric mouse systems (mo-s). **a.)** histograms of yields for the cluster types liquid (blue), open 6-stars (pink) and chain/loops (yellow). See the main paper for the definitions of the cluster types. There is one histogram plot for each patch position Δ, the x-axis of each of these histograms denotes the interaction strength ϵ. **b.)** The heatmap summarizes all yield histograms through mapping the yield distributions for each (Δ, ϵ) to a barycentric color triangle. **c.)** The barycentric color triangle for mo-as.

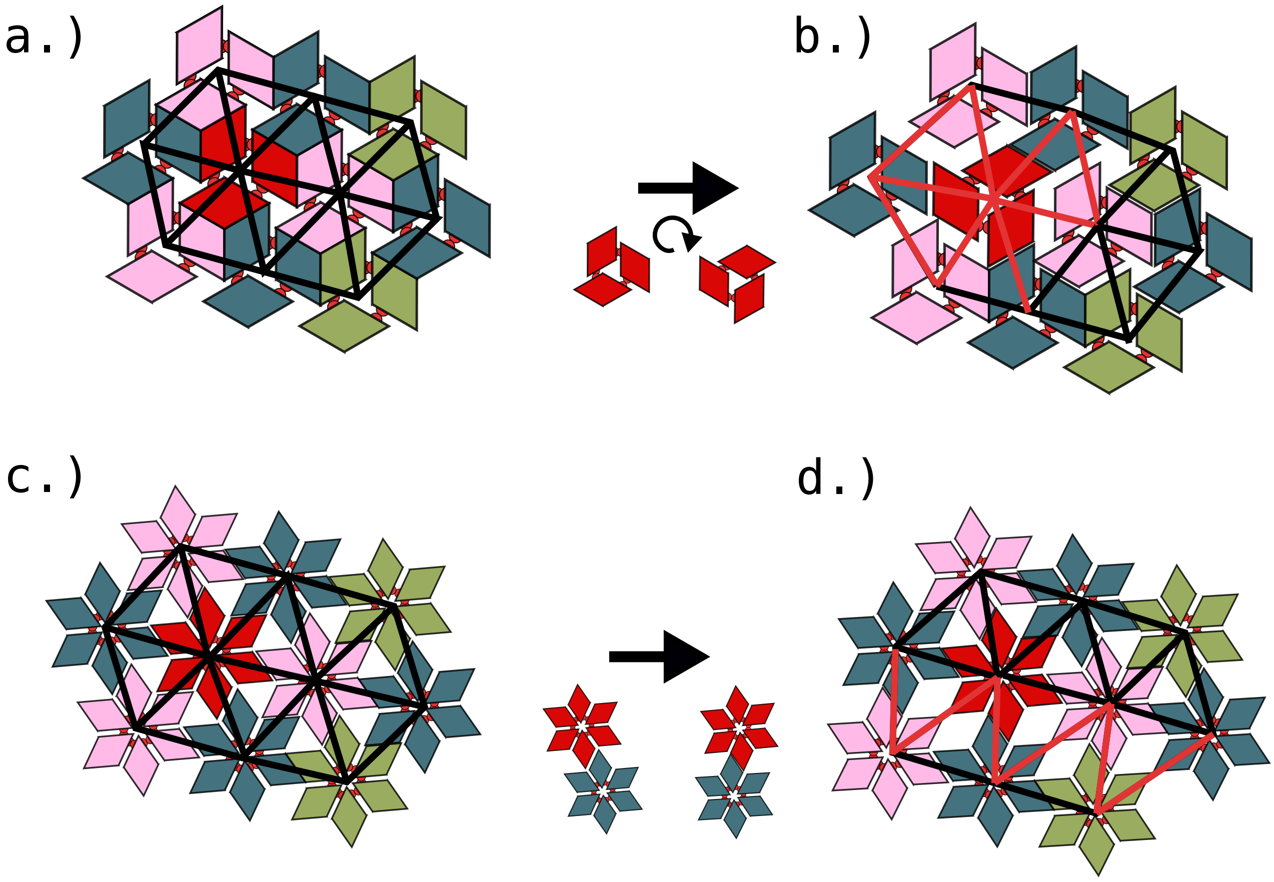

FIG. 5: Sketches of perfect lattices of open boxes and stars and their respective lattice defects. **a.)** Open tiling with triangular pores (ot-tiling) composed of open boxes. All open boxes, including the red box are in their correct lattice positions and orientations. The black lines connect the center positions of the open boxes and highlight the hexagonal order of the tiling. **b.)** The red open box is rotated by 60° with respect to the perfect ot-tiling in a.). Due to the rotation the rhombi of the red open box are now aligned parallel with their neighbouring rhombi, and hence the center-to-center distances change and the lattice gets distorted. Neighbouring boxes in correct lattice positions are still connected by black lines, while boxes that had to shift due to the orientational defect are now connected with red lines. **c.)** Open lattice with triangiular pores (ot-tiling) made of 6-stars. All stars, including the red star reside in their correct lattice positions. The hexagonal order of the star centers is highlighted by the black lines connecting the center positions. **d.)** The red star shifts to align one rhombi on the other edge of its neighbouring rhombi. This results in a line defect where all rhombi in the same line are forced to shift as well. The changed center-to-center distance lines are shown in red, while the lines connecting neighbours that maintain the correct lattice positions are still black.

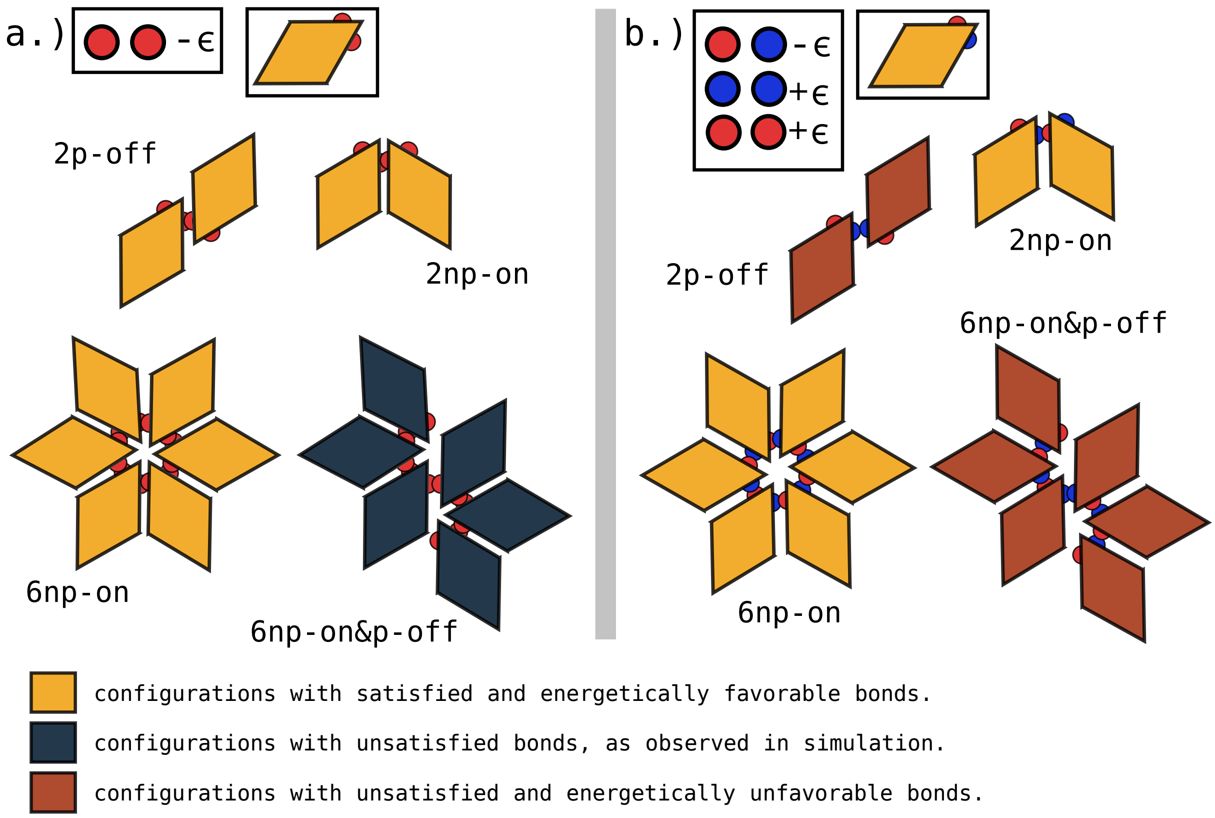

FIG. 6: Sketches of patch specificities favouring or disfavouring parallel two particle bonds (p-bonds) and subsequently broken stars. **a.)** Mouse rhombi with attractive patches of the same kind at $\Delta < 0.5$, where stars are prevalent. Parallel (2p-off) as well as non parallel (2np-on) bonds are allowed (both in yellow). Stars (6np-on) as well as broken stars with dangling bonds (6np-on&p-off, in dark blue) can form. **b.)**: Mouse rhombi with two kinds of patches where patches of the same kind repel each other and patches of differing kinds attract each other. Patches are positioned at $\Delta < 0.5$, for which stars have been observed. With this specificity 2p-off bonds are not allowed (in burgundy) while 2np-on are still possible (in yellow). This leads to broken stars becoming not allowed (6np-on&p-off, in burgundy) while stars are still allowed (6np-on, in yellow).